


RESEARCH

Open Access



# Microbiota-derived 3-phenylpropionic acid promotes myotube hypertrophy by Foxo3/NAD<sup>+</sup> signaling pathway

Penglin Li<sup>1†</sup>, Xiaohua Feng<sup>1†</sup>, Zewei Ma<sup>1</sup>, Yexian Yuan<sup>1</sup>, Hongfeng Jiang<sup>1</sup>, Guli Xu<sup>1</sup>, Yunlong Zhu<sup>1</sup>, Xue Yang<sup>1</sup>, Yujun Wang<sup>1</sup>, Canjun Zhu<sup>1</sup>, Songbo Wang<sup>1</sup>, Ping Gao<sup>1</sup>, Qingyan Jiang<sup>1,3,4\*</sup> and Gang Shu<sup>1,2,4\*</sup> 

## Abstract

**Background** Gut microbiota and their metabolites play a regulatory role in skeletal muscle growth and development, which be known as gut-muscle axis. 3-phenylpropionic acid (3-PPA), a metabolite produced by colonic microorganisms from phenylalanine in the gut, presents in large quantities in the blood circulation. But few study revealed its function in skeletal muscle development.

**Results** Here, we demonstrated the beneficial effects of 3-PPA on muscle mass increase and myotubes hypertrophy both in vivo and vitro. Further, we discovered the 3-PPA effectively inhibited protein degradation and promoted protein acetylation in C2C12 and chick embryo primary skeletal muscle myotubes. Mechanistically, we supported that 3-PPA reduced NAD<sup>+</sup> synthesis and subsequently suppressed tricarboxylic acid cycle and the mRNA expression of SIRT1/3, thus promoting the acetylation of total protein and Foxo3. Moreover, 3-PPA may inhibit Foxo3 activity by directly binding.

**Conclusions** This study firstly revealed the effect of 3-PPA on skeletal muscle growth and development, and newly discovered the interaction between 3-PPA and Foxo3/NAD<sup>+</sup> which mechanically promote myotubes hypertrophy. These results expand new understanding for the regulation of gut microbiota metabolites on skeletal muscle growth and development.

**Keywords** 3-Phenylpropionic acid, Gut microbiota metabolites, Muscle hypertrophy, NAD<sup>+</sup>, Acetylation

<sup>†</sup>Penglin Li and Xiaohua Feng have Contributed equally to this work.

\*Correspondence:

Qingyan Jiang  
qyjiang@scau.edu.cn

Gang Shu  
shugang@scau.edu.cn

<sup>1</sup> State Key Laboratory of Swine and Poultry Breeding Industry, Tianhe District, 483 Wushan Road, Guangzhou 510642, Guangdong, China

<sup>2</sup> Guangdong Laboratory for Lingnan Modern Agricultural and Guangdong Province, Tianhe District, 483 Wushan Road, Guangzhou 510642, Guangdong, China

<sup>3</sup> National Engineering Research Center for Breeding Swine Industry, College of Animal Science, South China Agricultural University, Tianhe District, 483 Wushan Road, Guangzhou 510642, Guangdong, China

<sup>4</sup> Key Laboratory of Animal Nutritional Regulation, College of Animal Science, South China Agricultural University, Tianhe District, 483 Wushan Road, Guangzhou 510642, Guangdong, China



## Introduction

As a crucial component of human body, skeletal muscle not only plays a major role in locomotor activity but also in metabolic homeostasis, energy consumption and protein storage [1]. Skeletal muscle development can be simply divided into three parts: the proliferation and the formation of myofibers, myotube hypertrophy and the repair of myotube injury, which are subject to the regulation of energy homeostasis, muscle angiogenesis [2], protein turnover and so on. The hypertrophy process jointly regulated by multiple signaling pathways, among which phosphatidylinositol 3-kinase (PI3K)/AKT/mTOR is the classical signaling pathway regulating protein synthesis in skeletal muscle. And Foxo family, a classical signaling pathway in protein degradation [3], is a class of transcriptionally active regulators whose activity is influenced by numerous upstream signaling molecules and is also regulated by post-translational modifications of proteins. Moreover, Foxo3 targets several myogenic transcription factors [4, 5] and protein degradation-related genes, and recently some new effectors with Foxo3 had appeared in promoting muscle hypertrophy [5, 6] and inhibiting muscle atrophy [7–9]. SIRT1/3 is a member of NAD-dependent deacetylases family, that could modify Foxo3 cytosolic location and regulate its binding to target genes [10, 11] to modulate cell energy expenditure [5]. Interestingly, Foxo3 can modulate SIRT/NAD<sup>+</sup> at transcriptional level that formed as a feedback regulation. However, there still are few studies explored the combination function of SIRT and Foxo3 in skeletal muscle development.

Recent years the gut-muscle axis, which refers to the composition of gut microbiota and their metabolites on skeletal muscle metabolism and functionality [12], has been gained wide attention. Germ-free mice that lack gut microbiota exhibited signs of muscle atrophy, mitochondria dysfunction and metabolic mode switching in muscle [13–15]. And microbiota metabolites, such as secondary bile acids, short-chain fatty acids [16] and microbial aromatic amino acids [17–19] could improve C2C12 proliferation, skeletal muscle mass and protein metabolism by influencing the glucose uptake and mitochondria function of skeletal muscle. Among lots of microbiota metabolites, 3-phenylpropionic acid (3-PPA) metabolizes from phenylalanine which is one of essential aromatic amino acids. Through LS-MA analysis, 3-PPA be found as the third substantially produced metabolites by colon microbiota in pigs that be ranked behind short-chain fatty acid and lithocholic acid [17, 20]. At present, the reports about 3-PPA is still shallow, mainly be relevant to its function in regulating insulin secretion after the intake of glucose and jointly maintaining blood glucose balance [21, 22] via G-protein-coupled receptor 40 which can express in C2C12 myotubes. Based on those,

the function of 3-PPA in regulating skeletal muscle development still unclear.

In this study, we reported that 3-PPA significantly increase the myotubes diameter by restraining protein degradation instead of protein synthesis. By using siRNA interference and immunoprecipitation, we found that 3-PPA inhibited NAD<sup>+</sup> synthesis and tricarboxylic acid cycle, decreased the mRNA expression of SIRT1/3, which facilitates the acetylation of total protein and Foxo3. Moreover, we demonstrated that 3-PPA also can inhibit Foxo3 protein expression in C2C12 nuclei by direct binding through AutoDock software and CETSA assay. Overall, our findings provided a new understanding of the function and the mechanism of microbiota metabolites on skeletal muscle development.

## Materials and methods

### Cell culture

The mouse myoblast cell line C2C12 (ATCC, RRID: CVCL\_0188) was cultured in high glucose DMEM (GIBCO, Grand Island, NY, USA) with penicillin (100 U/mL), fetal bovine serum (10%) and streptomycin (100 µg/mL) at 37 °C, in a humidified atmosphere containing 5% CO<sub>2</sub>. When cells got 90% confluency, culture media was switched by DMEM with 2% horse serum to induce myoblast differentiation to myotubes for 6 days.

### Primary chicken embryos skeletal muscle cells extraction

The leg muscle tissues of 10-embryo-old chicken embryos were collected, and the bones, mucous membranes and skin tissues were removed with surgical scissors and forceps. The muscle tissues were cut to the shape of minced meat, then digested with the addition of trypsin in the incubator at 37°C for 15~20 min (repeat blowing for 5-6 times) and terminated the digestion with complete medium (20% fetal bovine serum and 0.5% penicillin, streptomycin in high-sugar DMEM) to terminate digestion. After filtration with a 70 µm filter, the cells were centrifuged at 1500 r/min for 5 min, resuspended in complete medium, transferred to culture dishes, and wall-applied twice to obtain purified myoblasts. The purified cells were placed in the incubator at 37 °C with 5% CO<sub>2</sub>.

### Puromycin incorporation

Myotubes were incubated with puromycin at a concentration of 1 µg/mL after the end of 3-phenylpropionic acid treatment for 1 h. At the end of the incubation, the cell plates were washed three times with PBS, and the proteins were extracted and subjected to the Western Blot assay. Exposure was performed using FluorChem M Fluorescent Imaging System (Protein Simple, San

Jose, CA, USA); the images obtained after exposure were counted in grey scale by ImageJ software.

#### **NAD<sup>+</sup>/NADH/Acetyl-CoA/Glucose/Lactic acid content detection**

The NAD<sup>+</sup>/NADH content assay kit was purchased from Beyotime Biotechnology (S0175); The Acetyl-CoA content assay kit was purchased from Solarbio(BC0980); Glucose and lactic acid content test kits were purchased from Nanjing Jianjian Bioengineering Institute (F006-1-1, A019-2-1). These assays were performed along with those kit instructions.

#### **Foxo3 siRNA transfection**

The transfection steps and siRNA sequences of Foxo3 was described in our previous study. The siRNA of Foxo3 was purchased from Guangzhou RiboBio Co., Ltd (Guangzhou, China) and transfected with lipofectamine (Invitrogen, Carlsbad, CA, USA) followed by the manufacturer's instructions.

#### **Immunoprecipitation**

Immunoprecipitation was performed with Protein G Dynabeads(10003D,Thermo Fisher Scientific). The Dynabeads were reacted with rabbit anti-Foxo3 (A0102, ABclonal), Pan-acetylation (66289-1-Ig, Proteintech) and Histone H3 (4499S, CST) and rabbit anti-IgG (Normal IgG, CST) for 4 h at room temperature washed with buffer solution for three times. The Dynabeads were incubated with equal amounts of total or fractionated protein extracts overnight at 4 °C in a vertical mixing rotator, washed with buffer solution three times, and collected the Dynabeads. The Supernatant collection is used as input control. The collected Dynabeads were denatured at 100 °C for 10 min with 2xSDS-PAGE buffer, and stored in - 20 °C until the Western blot assay as the previous methods.

#### **Western blot analysis**

Cells or muscles were cracked by the RIPA lysis buffer containing 1 mM PMSE. For the nuclear or cytoplasmic protein extraction, the procedure of protein extraction was followed by the nuclear extraction kit (BB3112, Bestbio). Protein concentration was detected by a BCA protein assays kit. After sodium dodecyl sulfate (SDS) polyacrylamide gel electrophoresis gels, total protein lysates (20 µg) were immunoblotted with primary antibody (P-Foxo3: AP0684, ABclonal; Foxo3: A0102, ABclonal; P-mTOR: 5536S, CST; mTOR: ab185696, Abcam; P-AKT, 4071S, CST; AKT: 9272S, CST; Ubiquitin: A2129, ABclonal; Puromycin: MABE343, EMD Millipore Corporation; P-JAK2: BS-2485R, Bioss; JAK2: 3230S, CST; P-STAT3: 9145S, CST; STAT3: 12640S, CST;

MyoD: sc-377460, Santa Cruz Biotechnology; MyoG: 382257, CST; MyHC: MAB4470, CST; Histone H3: 4499S, CST; Pan-acetylation: 66289-1-Ig, Proteintech; GPR43: sc-293202, Santa Cruz Biotechnology; followed by incubating with goat anti-rabbit or goat anti-mouse HRP-conjugated secondary antibody (1:50 000). The levels of GAPDH, VDAC and β-actin served as the loading control. Protein expression levels were determined using MetaMorph software ImageJ (National Institutes of Health, USA).

#### **RNA extraction, reverse transcript, and qPCR**

Total RNA from cells was extracted by using an RNA extraction kit (Guangzhou Magen Biotechnology Co., Ltd, China) and Trizol reagent (Invitrogen, Carlsbad, CA, USA) according to the manufacturer's instructions. The total RNA was retrotranscribed into cDNA by 4xReverse Transcription Master Mix (A0010GQ) according to protocol of the kit. Using the designed primers, 2xSYBR Green qPCR Master Mix (ROX2 Plus) (A0001-R2) was used in accordance with the stated procedures. cDNA synthesis was performed with the Applied Biosystems QuantStudio 3 Real-Time PCR System. The primers sequences used for PCR are provided in Table 1.

#### **Immunofluorescence staining**

For staining of C2C12 cell, C2C12 cell was punched in 0.4% Triton for 10 min and then blocked for 1 h with a slowly shaking at room temperature. The sections were then incubated with primary antibody at room temperature overnight in a wet box. Goat anti-rabbit FITC (bs-0295G, Bioss), goat anti-mouse IgM/Alexa Fluor 555 antibody (bs-0368G-AF555, Bioss), goat anti-rabbit Flour 555 (bs-0295G, Bioss), goat anti-mouse FITC (bs-50950, Bioworld), rabbit anti-goat IgG FITC (bs-0294R, Bioss), and corresponding second antibodies were supplied for use. A Nikon Eclipse Ti-s microscope was used to take photos of these sections. Images of fluorescent intensity were analyzed with Nis-Elements BR software (Nikon Instruments, Tokyo, Japan).

#### **CCK-8 and EdU incorporation Assay**

An appropriate number of cells were cultured in a 96-well plate. After culturing the cell overnight and returning to normal, the required drug or other stimulation treatment was performed. Then CCK-8 detection was carried out. While for the EdU incorporation assay, cells were incubated with EdU reagent at 37 °C for 2 h and were then fixed in 4% paraformaldehyde for 15 min and washed with PBS 3 times (5 min each). After that, cells were permeabilized with 0.3% Triton X-100 for 10 min and washed with PBS before adding a click additive solution for 30 min. The nuclei were stained with Hoechst,

**Table 1** QPCR primer sequence

Gene	Forward primer sequence (5'-3')	Reverse primer sequence (5'-3')
DRP1	GCAACTGGAGAGGAATGCTG	CACAATCTCGCTGTTCTCGG
ATP5A1	GTTTCAACGATGGGACCGAC	TCCGTCAGTCTCTTACCAG
COX6A1	TGCTCAACGTGTTCTCAAG	TAAGGGTCCAAAACCACTGC
TFAM	AGATATGGGTGTGGCCCTTG	AAAGCCTGGCAGCTTCTTTG
NDUFA6	CAAGATGGCGGGGAGCGG	GTATAGTGAGTTTATTTGTGCTC
PGC1- $\alpha$	TCAGAACCATGCAGCAAACC	TTGGTGTGAGGAGGGTCATC
SIRT1	TCCTTGGAGACTGCGATGTT	AATTCCTTTTGTGGCGTGG
PINK1	CGAGCATCTTCTAGCCCTGA	TTCTCTCTCAGCCTGTCAGC
BNIP3	TCCAGCCTCCGTCTCTATTTA	TGGTATCTTGTGGTGTCTGGG
PARK2	ACAAATGCATCTGGAGGGGA	ACCTCTGGCTGCTTCTGAAT
SQSTM1	ACATGGAGGGAAGAGAAGCC	CACCGACTCCAAGGCTATCT
ATG5	GCCATCAACCGAAAACATCAT	GATCTCCAAGTGTGTGCAGC
ATG7	GGGGTTTTCTGTCACGGTTC	AGCAGCTTGGGTCTCTTGAT
VDAC	GGCTCACCTTCAACCCAAAAG	GCCGAGACTAAAACAATCCCG
Ndufb8	AAGACTACGAGCCATACCCC	GGTCCCAGTGTATCGGTTCA
SDHB	CTGTCTGAGGGGCACAGAC	CAACACCATAGGTCCGCACT
NAMPT	TGATCCCAACAAAAGGTGCGAA	CCCCTCACACAAAAGCCTA
NMNAT2	AGAACACCCAGCCCATTTAC	GAGGCTTTCTCCACCTTTC
SIRT3	CAGCTACATGCACGGTCTGT	ACACAATGTCGGGTTTCACA
UQCRC1	TTCAGCAATTTAGGAACCC	GGTCACACTTAATTTGCCACCAA
CS	CGTTTCCGAGGTCATAGTATCCC	GCTGAGACATAGGGTGTAGGTTGG
IDH2	CCCGTATTATCTGGCAGTTCATC	ATCAGTCTGACGGTTTGG
OGDH	GCCACCACCACTTTCATC	CCGCTTCTCCTCGTTGGT

and images were captured with a Nikon Eclipse Ti-s microscope (Nikon Instruments, Tokyo, Japan).

### Molecular docking

The crystal structure of the Foxo3 and GPR40 protein was downloaded from the Protein Data Bank ([www.rcsb.org](http://www.rcsb.org)). The GPR40 was used as a control which is regarded as ligand of 3-PPA. The structure of 3-PPA was downloaded from ZINC ([zinc.docking.org](http://zinc.docking.org)). All the steps during docking followed by the video ([www.bilibili.com](http://www.bilibili.com)). We use PyMOL software to visualize the docking result and calculate the binding energy, ligand efficiency and so on.

### Cellular thermal shift assay (CETSA)

CETSA experiments were performed according to a recording protocol [23]. C2C12 cells were treated with PBS or 3-PPA. After incubation for 2 h, the cells were washed with PBS, harvested by RIPA. Protein concentration was detected by a BCA protein assays kit. Equal amounts of cell suspensions were aliquoted into 0.2 mL PCR microtubes. Subsequently, the cell suspension aliquots were heated individually at different temperatures for 3 min (GE9612T, BIO-GENER), followed by cooling for 5 min at room temperature. Then, the soluble fractions were isolated by centrifugation and analyzed by

SDS-polyacrylamide gel electrophoresis (SDS-PAGE) followed by western blot as described above. Fold-changes in the immunoblot band densities (normalized to the GAPDH and using the lowest temperature condition as reference) were plotted as a function of temperature to generate foxo3 melt curves for the different treatments.

### Statistics

Statistical analyses were using GraphPad Prism 9.0 software (Chicago, IL, USA). Methods of statistical analyses were chosen based on the design of each experiment and are indicated in the figure legends. The data are presented as mean  $\pm$  SEM.  $P < 0.05$  was statistically significant.

## Results

### 3-PPA increases muscle mass in mice and induces hypertrophy in C2C12 myotubes

To explore the influence of 3-PPA on growth and body composition in mice, 6 week-old C57BL/6 male mice were treated with water containing 0.5% 3-PPA for 7 weeks. During this process, we found 3-PPA significantly increase the body weight gain (Fig. 1a), the lean mass and gastrocnemius weight were promoted after 6 weeks' treatment (Fig. 1b, c). Consistently, 3-PPA can prompt muscle fiber cross-section area in Gastrocnemius

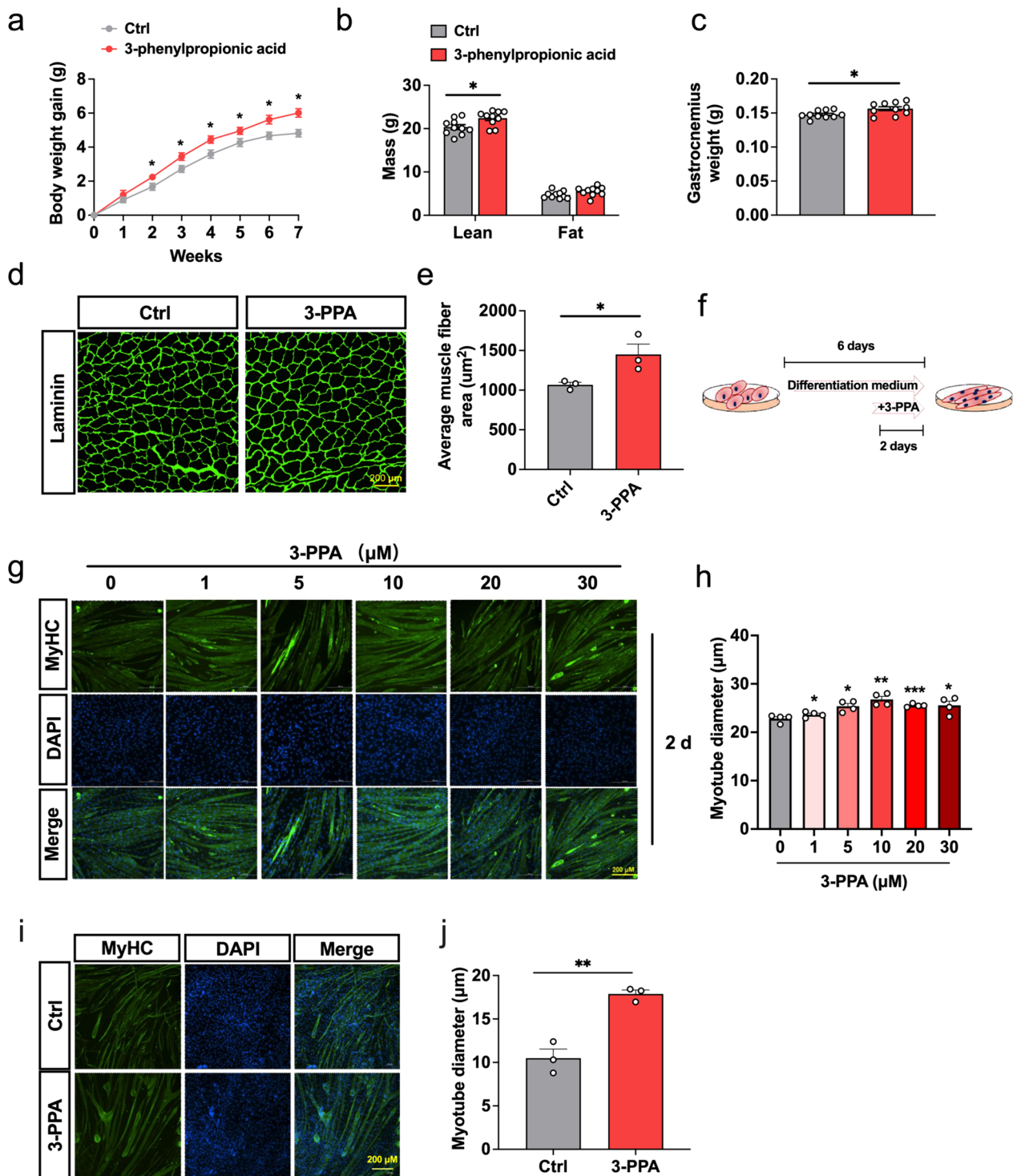


**Fig. 1** Effect of 3-PPA on muscle mass and C2C12 myotubes hypertrophy. **a** Body weight gain in 6 week-old male mice with 7 weeks' treatment of 0.5% 3-PPA (n = 10). **b** Lean mass and fat mass of mice after 6 weeks' treatment of 3-PPA by QMR (n = 10). **c** Gastrocnemius weight of mice after 7 weeks' treatment (n = 10). **d–e** The laminin immunofluorescent staining (**d**) and frequency histogram of gastrocnemius muscle fiber cross-sectional area statistical analysis (**e**) in C57BL/6 male mice after 3 weeks 3-PPA treatment (n = 3). **f** Schematic representation of C2C12 treated with 3-PPA for 2 days. **g–h** Immunofluorescence images (**g**) and statistics of myotube diameter (**h**) of C2C12 myotubes in 3-PPA treatment for 2 days (n = 4). **i–j** Immunofluorescence images (**i**) and statistics of myotube diameter (**j**) of chick embryo primary skeletal muscle cells in 3-PPA treatment for 2 days (n = 3)

muscle of mice (Fig. 1d, e). Further, we investigated the affection of 3-PPA in skeletal muscle *in vitro* by detecting C2C12 proliferation, differentiation and myotube hypertrophy. As shown in CCK-8 and EdU assay (Fig S1a-c), 3-PPA has no effects on the proliferation activity of C2C12 in various concentration and time. Then, we added 3-PPA in differentiation medium at differentiation day 1 and day 4 respectively. The results showed that 3-PPA significantly increase myotube diameter in 2 days treatment (Fig. 1f-h) instead of 6 days (Fig S1d-f). What's more, 3-PPA performed the same function in chick-embryo primary skeletal muscle cells (Fig. 1i, j). Taken this together, Fig. 1 indicates that 3-PPA has

important role in promoting muscle mass and myotube hypertrophy.

### 3-PPA attenuated protein degradation instead of protein synthesis in C2C12 myotubes

Muscle hypertrophy that performed as increased muscle nuclei and thickened muscle fibers impinge on excessive protein synthesis and reduced protein degradation [24]. To examine the mechanism of myotube hypertrophy caused by 3-PPA treatment, we firstly evaluated the 3-PPA's effects in protein degradation and synthesis. As shown in Fig. 2c, d, we found 3-PPA suppressed ubiquitin levels of total protein, which mainly take charge of

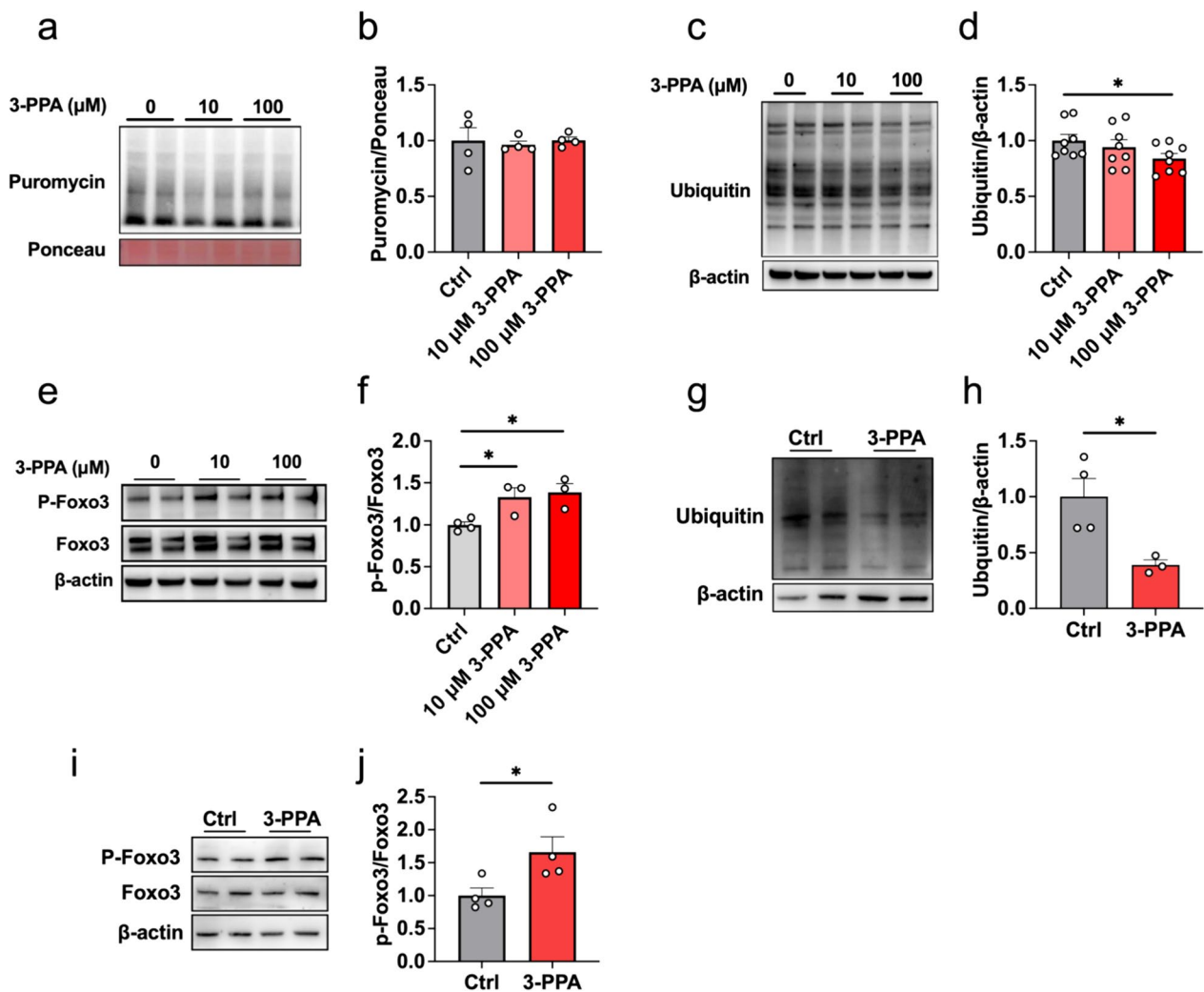


**Fig. 2.** 3-PPA attenuated protein degradation instead of protein synthesis in C2C12 myotubes. **a–b** Immunoblots (**a**) and quantification (**b**) of the puromycin-labeled protein expression of C2C12 myotubes with 3-PPA treatment for 2 days ( $n=8$ ). **c–d** Immunoblots (**c**) and quantification (**d**) of total ubiquitination protein expression of C2C12 myotubes with 3-PPA treatment for 2 days ( $n=4$ ). **e–f** Immunoblots (**e**) and quantification (**f**) of P-Foxo3 and Foxo3 protein expression of C2C12 myotubes with 3-PPA treatment ( $n=3$ ). **g–h** Immunoblots (**g**) and quantification (**h**) of the total ubiquitination protein expression of chick embryo primary skeletal muscle myotubes with 3-PPA treatment for 2 days ( $n=3-4$ ). **(i–j)** Immunoblots (**i**) and quantification (**j**) of P-Foxo3 and Foxo3 protein expression in chick embryo primary skeletal muscle myotubes ( $n=4$ )

protein degradation [25], but has no effects in the expression of puromycin-labeled protein which on behalf of the rate of protein synthesis (Fig. 2a, b). Subsequently, the phosphorylation of Foxo3, which could inhibit multiple constituents of ubiquitination of protein and muscle wasting [26], was significantly increased (Fig. 2e, f). The results in chick embryo primary skeletal muscle cells were further verified the effect of 3-PPA (Fig. 2g-j). However, the protein expression of JAK/STAT3, AKT/mTOR [27] and ERK pathway which are related to regulating protein synthesis and degradation were didn't change (Fig S2). Taken together, we found that 3-PPA has effects on inhibiting protein degradation but no protein synthesis, which may induce protein deposition and myotube hypertrophy.

#### Protein acetylation modification mediates the effect of 3-PPA on myotube hypertrophy.

Since energy supply are crucial for myotube hypertrophy, we speculated that 3-PPA may promote myotube hypertrophy by affecting myotube energy metabolism. Our results showed that 3-PPA had no effect on the contents of glucose, lactic acid and reactive oxygen species which were metabolites produced by glycolysis and aerobic oxidation, but significantly reduced the content of ATP in myotubes (Fig. 3a-d). Mitochondria are the “factories” of energy creation in the body, their quantity and function directly affect the metabolic level of the body. As shown in Fig. 3e, f, 3-PPA had no effect on the expression of genes related to mitochondrial fusion and formation, but significantly inhibited the gene expression of mitochondrial autophagy markers (PINK1 and BNIP3) and NADH: Ubiquinone Oxidoreductase Subunit B8 (NDUFB8) and proved NDUFA6 gene expression. The tricarboxylic acid cycle is the main way for the body to obtain energy on the mitochondrial matrix. The results of qPCR showed that 3-PPA significantly inhibited the gene expressions of citrate synthetase (CS) and ketoglutarate dehydrogenase (OGDH) in the tricarboxylic acid cycle (Fig. 3g), along with the increase of acetyl-CoA content (Fig. 3h) and the acetylation level of total protein (Fig. 3i, j) in myotubes. To verify whether acetylation of protein mediates 3-PPA's

function, acetyltransferase inhibitor C646 was added to detect the myotube diameter, as shown in Fig. 3k, l, C646 was able to successfully reverse the effect of 3-PPA on promoting the myotube diameter. It's reported that the  $NAD^+/NADH$  ratio control the rate of tricarboxylic acid cycle, we found 3-PPA had a significant inhibitory effect on the  $NAD^+/NADH$  ratio (Fig. 3m), and the mRNA expression of nicotinamide phosphoribosyltransferase (NAMPT) which is crucial to  $NAD^+$  synthesis (Fig. 3n). SIRT is a class of  $NAD^+$ -dependent protein deacetylase, and 3-PPA also significantly inhibited the mRNA expression of SIRT1 and SIRT3 genes (Fig. 3o), consistent with the results of 3-PPA in accumulating the content of acetyl-coA in the C2C12 myotubes. Taken together, 3-PPA promotes acetyl-CoA content and acetylation modification by reducing the rate of tricarboxylic acid cycle and SIRT1/3 mRNA expression, which may suppress protein degradation and induce myotube hypertrophy.

#### Foxo3/ $NAD^+$ /Acetylation pathway is required for 3-PPA to increase protein acetylation modification.

Further, we wonder if Foxo3 could correlated with acetyl-CoA in playing the function of 3-PPA., Immunofluorescence analysis of Foxo3 revealed lower activity of the translocation between nuclei and cytoplasm (Fig. 4c, d), which is consistent with the decreased levels of nuclei and cytoplasm protein in immunoblotting result (Fig. 4a, b). In order to further verify the role of Foxo3 protein in the promotion of myotubes hypertrophy by 3-PPA, three siRNA sequences were used to interfere with Foxo3 protein expression, among which siRNA-3 has a significant inhibitory effect (Fig. 4e, f). After siRNA-3 treatment, the effect of 3-PPA on the myotube diameter disappeared (Fig. 4g, h). It has been shown that Foxo3 activity is directly regulated by  $NAD^+$  and SIRT1, and  $NAD^+$  synthesis related NAMPT gene is the target gene of Foxo3 protein at the same time. Consistently, we observed a decrease in NAMPT mRNA expression after knocking down Foxo3 expression (Fig. 4i). Acute activate of NAMPT activity with the specific agonist P7C3 significantly reverse the inhibitory effect

(See figure on next page.)

**Fig. 3** Protein acetylation modification mediates the effect of 3-PPA in myotube hypertrophy. **a-d** The glucose content (**a**), LD content (**b**), ATP content (**c**), ROS content (**d**) in C2C12 myotubes with 3-PPA treatment for 2 days (n=3 to 4). **e** Mitochondria biogenesis and function related gene mRNA expression in C2C12 myotubes with 3-PPA treatment for 2 days (n=4 to 8). **f** Mitochondria autophagy related gene mRNA expression in C2C12 myotubes with 3-PPA treatment for 2 days (n=4). **g** Tricarboxylic acid cycle related gene mRNA expression in C2C12 myotubes with 3-PPA treatment for 2 days (n=6). **h** Relative Acetyl-CoA content in C2C12 myotubes with 3-PPA treatment for 2 days (n=6). **i-j** Immunoblots (**i**) and quantification (**j**) of Pan-acetylation protein expression of C2C12 myotubes with 3-PPA treatment for 2 days (n=3). **k-l** Immunofluorescence images (**k**) and statistics of myotube diameter (**l**) of C2C12 myotubes in C646 and 3-PPA co-treatment (n=3). **m** The ratio of  $NAD^+/NADH$  in C2C12 myotubes with 3-PPA treatment for 2 days (n=3). **n** mRNA expression of NAMPT and NAMPT in C2C12 myotubes with 3-PPA treatment for 2 days (n=6). **o** mRNA expression of SIRT1 and SIRT3 in C2C12 myotubes with 3-PPA treatment for 2 days (n=6)

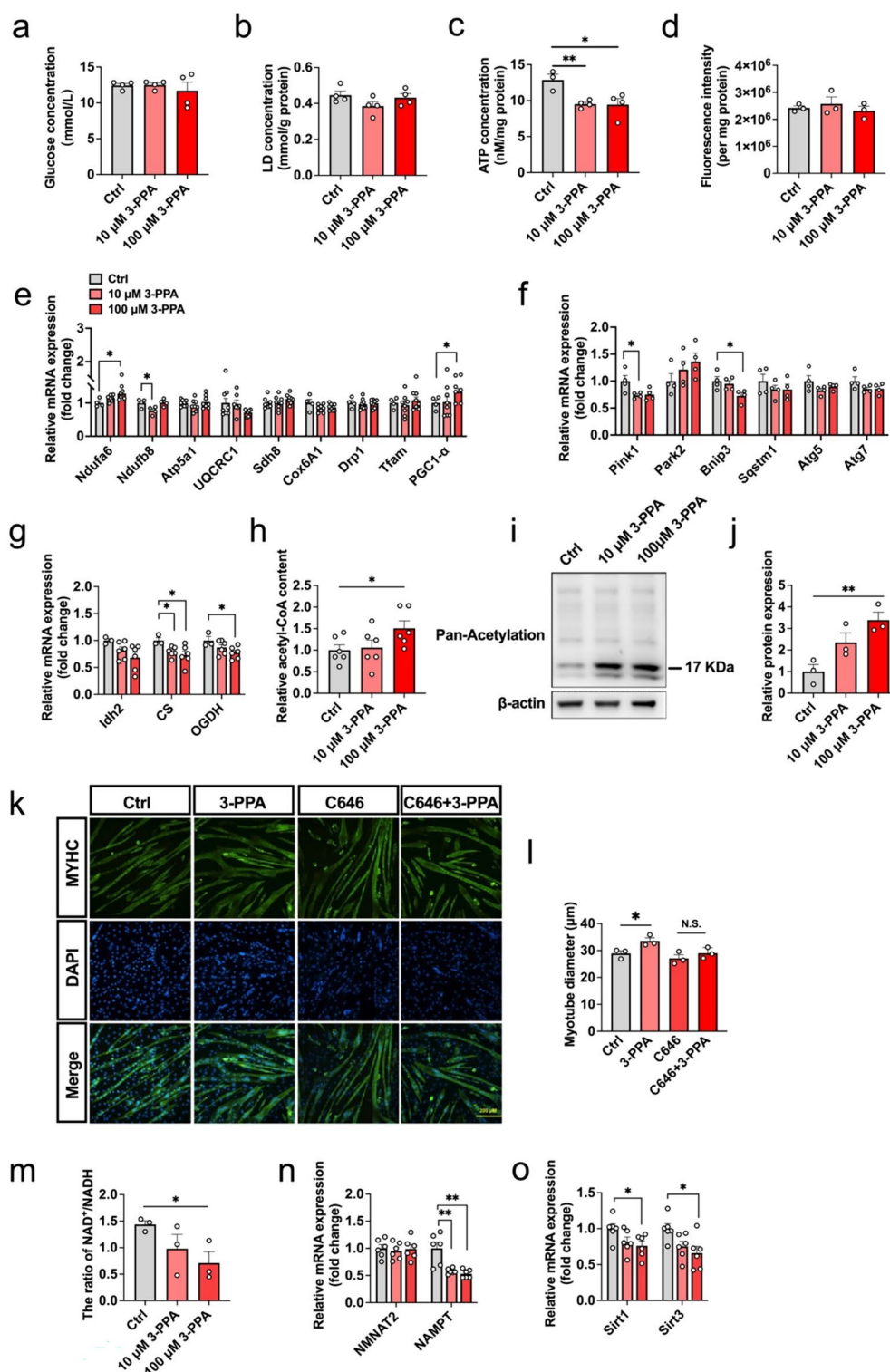


**Fig. 3** (See legend on previous page.)

3-PPA in Foxo3 (Fig. 4j, k). What’s more, 3-PPA treatment triggered the acetylation of endogenous Foxo3 which causes inactive of Foxo3 protein (Fig. 4l, m), and

acetyltransferase inhibitor C646 successfully altered this situation (Fig. 4n, o). Subsequently, we wonder if 3-PPA inhibits Foxo3 activity by directly binding. To figure this



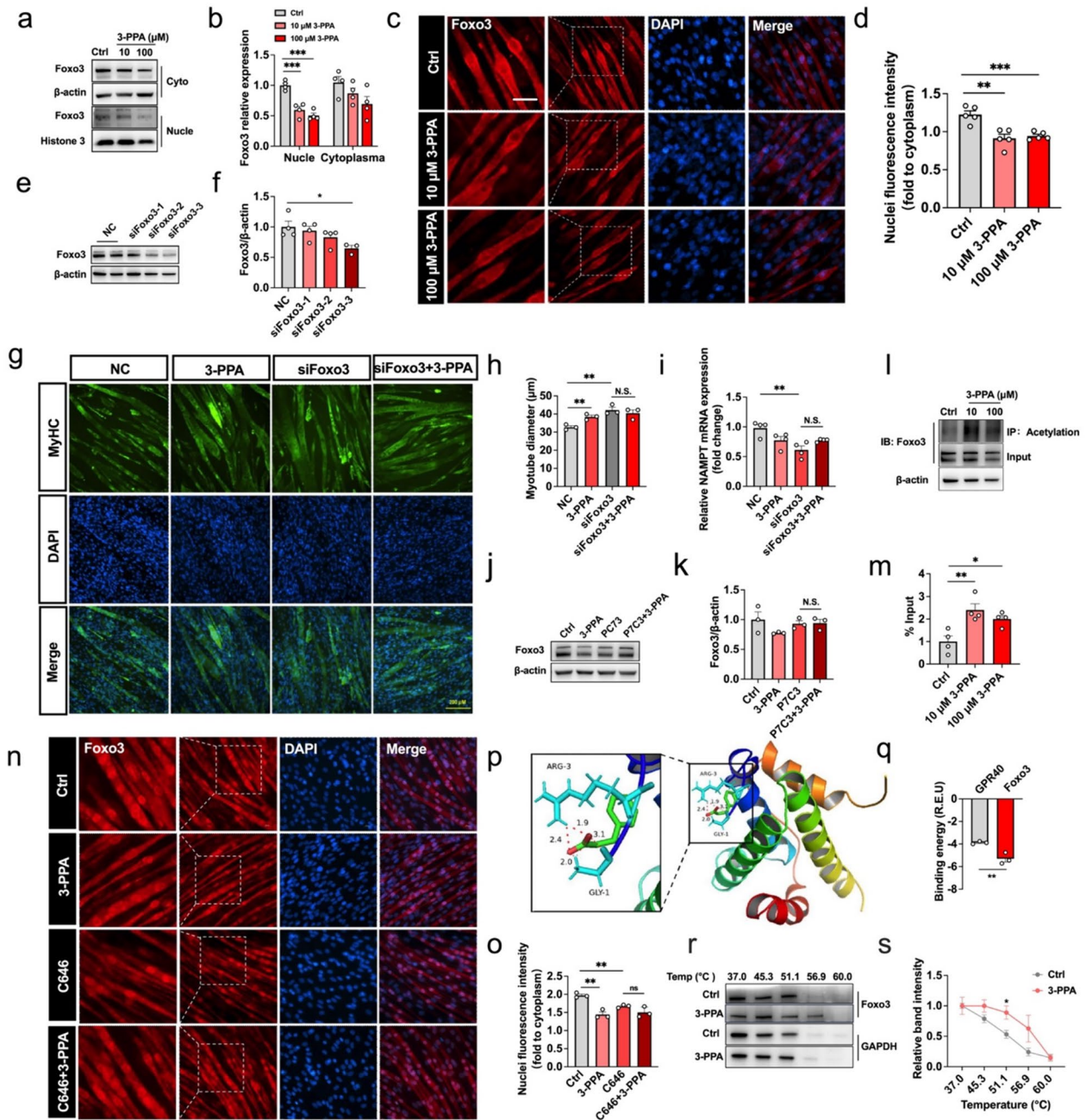


**Fig. 4** Foxo3/NAD<sup>+</sup> pathway is required for 3-PPA to increase protein acetylation modification. **a–b** Immunoblots (**a**) and quantification (**b**) of Foxo3 protein expression in nuclei and cytoplasm of C2C12 myotubes with 3-PPA treatment for 2 days (n=4). **c–d** Immunofluorescence images (**c**) and statistics (**d**) of relative nuclei Foxo3 protein in C2C12 myotubes in 3-PPA treatment for 2 days (n=3). **e–f** Immunoblots (**e**) and quantification (**f**) of Foxo3 protein expression in C2C12 myotubes with different siRNA sequence treatment (n=3 to 4). **g–h** Immunofluorescence images (**g**) and statistics (**h**) of myotube diameter in C2C12 myotubes with siFoxo3 and 3-PPA co-treatment (n=3). **i** mRNA expression of NAMPT in C2C12 myotubes with si Foxo3 and 3-PPA co-treatment (n=4). **j–k** Immunoblots (**j**) and quantification (**k**) of Foxo3 protein expression in C2C12 myotubes with P7C3 and 3-PPA co-treatment (n=3). **l–m** Immunoprecipitation (**l**) and statistics (**m**) of Ace- Foxo3 in C2C12 myotubes with 3-PPA treatment for 2 days (n=4). **n–o** Immunofluorescence images (**n**) and statistics (**o**) of Foxo3 of C2C12 myotubes in C646 and 3-PPA co-treatment (n=3). **(p)** Binding region of 3-PPA and Foxo3 protein. **(q)** Calculated binding energy of Foxo3 and GPR40. **r–s** Immunoblots (**r**) and quantification (**s**) of relative Foxo3 protein expression in CETA assay by 3-PPA treatment (n=3)

out, AutoDock 4.0 software was used to simulate the docking between 3-PPA and Foxo3 protein. The results showed that the calculated binding energy of 3-PPA and Foxo3 protein was significantly stronger than that of 3-PPA and GPR40 (positive control group) (Fig. 4p, q). And the CETSA result consistently proved the direct binding by increasing the thermal stability of Foxo3 protein (Fig. 4r, s). It is therefore tempting to speculate that 3-PPA promotes acetylation of Foxo3 by the coordinated sequential actions of NAD<sup>+</sup> and SIRT1, and lower Foxo3 activity further inhibited NAD<sup>+</sup> synthesis, which generated a positive feedback loop regulation. Hence, these data support the hypothesis that 3-PPA may inhibit the activity of Foxo3 by directly binding, thus inhibiting NAMPT mRNA expression, and promoting protein acetylation and myotube hypertrophy in skeletal muscle through NAD<sup>+</sup>/SIRT signaling pathway. Meanwhile, the NAD<sup>+</sup>/SIRT signaling pathway can further regulate Foxo3 protein expression (Fig. 5).

## Discussion

The development of skeletal muscle is a complicated biological molecular process which involves cell proliferation, differentiation and myotube hypertrophy [28], which mainly regulated by myogenic regulatory factors [29], muscle-specific miRNAs [30], and so on. Recent reports have highlighted the role of gut microbiota and its metabolites shed light on skeletal muscle function, composition, and development [12–15]. IPA, a bioactive metabolite of *C.sporogenes*, promotes C2C12 proliferation by regulating the myogenic regulatory factor signaling [18]. Butyrate which produced by bacterial fermentation in the gut could alleviate skeletal muscle atrophy and enhance skeletal muscle mitochondrial function in the aging mice [31]. 3-PPA which is produced by

*Firmicutes*, *Bacteroidetes* and *Actinobacteria* from phenylalanine (one of aromatic amino acids) in colon [17, 32] has few reports in regulating skeletal muscle development, and function.

In this study, we first indicated that different concentrations of 3-PPA significantly increased C2C12 myotubes diameter and promoted myotube hypertrophy, but failed to affect the proliferation and differentiation of C2C12 and repaired the muscle injury. So, why does 3-PPA only influence the hypertrophy of myotubes? According to the simplistic view, the key function factors of myogenic transcription factors were different [33–35] and the morphology of myotubes is not the same during myotubes normal differentiation. After 3 days' differentiation when already existed primary myotubes [36], the muscle activity focus on the dynamically regulation of the protein synthesis and protein breakdown, which can be regulated by various molecules, such as AKT-mTOR, GPRs, ubiquitin-proteasome and so on [37, 38]. When 3-PPA added in whole process, we found the protein expression of MyoD and MyoG and the fusion index didn't change. But in latest 2 day's treatment, myotubes diameter significantly increased, and ubiquitination of total proteins inhibited. The distinct influence of 3-PPA in MRFs and protein degradation may take an explanation for its unique function in muscle hypertrophy. Also, the lack of detail study in proteasome and E1/E3 enzymes that are key biomarker in protein degradation needs complete in the future.

Energy metabolism of skeletal muscle affects the deposition and consumption of nutrients, regulating the skeletal muscle growth and development. Studies have found that secondary bile acids produced by intestinal microbial metabolism can activate downstream cAMP by binding with bile acid receptor 5 on skeletal muscle and increase skeletal muscle energy consumption [39]. Short-chain fatty acids can also participate in the transformation of skeletal muscle fibers from glycolysis to oxidation through regulation of AMPK activity, regulate the balance of body energy metabolism and improve endurance exercise ability [40]. Mitochondria are "energy factory", its biological function and respiratory activity is related with TCA cycle in skeletal muscle which occurs in the mitochondrial matrix is the center of energy metabolism to connecting the metabolism of three major nutrients. The NADH and FADH<sub>2</sub> produced by TCA cycle associated with the oxidative respiration transport chain to promote the generation of ATP from ADP [41], providing energy for the body's virtual activities. Our data showed that 3-PPA significantly decreased ATP content and NAD<sup>+</sup>/NADH ratio in the C2C12 myotubes, inhibited the gene expression of citrate synthase and ketoglutarate dehydrogenase, and restricted the TCA cycle. ATP

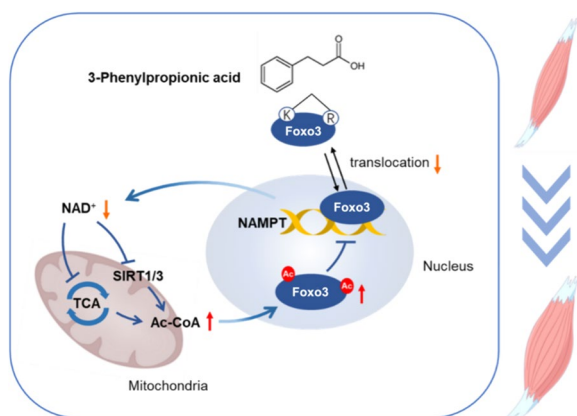


**Fig. 5** Schematic diagram of 3-PPA's function on myotube hypertrophy

has been regarded as an intracellular energy currency molecule in animal body, and the decrease of its content may indicate a vigorous stage of myotubes energy metabolism and a requirement for more ATP to consume. At the same time, we found that 3-PPA significantly inhibited the expression of genes related to mitochondrial autophagy but had no effect on the expression of genes related to mitochondrial fusion, generation and biological function. In conclusion, it is possible that 3-PPA can accelerate the growth rate of myotubes and increase the requirements of nutrient and energy. To maintain the normal level of ATP, PAKR2 and BNIP3 gene expressions are inhibited to reduce mitochondrial autophagy.

In addition to its important role of hydrogen and electron transfer in oxidation reduction and oxidative phosphorylation,  $\text{NAD}^+$  serves as a substrate for many metabolic enzymes, including SIRT, PARPs and DNA ligase [42]. NAMPT, the rate-limiting enzyme in the  $\text{NAD}^+$  salvage pathway [43], plays a crucial role in maintaining skeletal muscle development and mitochondria function. Skeletal muscle specific NAMPT knockout mice display muscle atrophy, mitochondria dysfunction and more centralized nuclei [44]. However, when NAMPT protein levels are decreased by approximately 14%, it had no significant effect on the expression of mitochondrial respiratory capacity in skeletal muscle [45]. This study found that 3-PPA significantly inhibited the expression of NAMPT gene and the content of  $\text{NAD}^+$ , but had no significant effect on the mitochondrial function in the C2C12 myotubes. Therefore, we suspect that 3-PPA might regulate the activity of some metabolic enzymes by inhibiting the synthesis of  $\text{NAD}^+$  to promote myotube hypertrophy rather than affecting mitochondrial oxidative phosphorylation and electron transport chains.

SIRT, which use  $\text{NAD}^+$  as a co-enzyme, regulate protein activity, chromatin stability and gene transcription by catalyzing histone and non-histone deacetylation, and participate in physiological and biochemical processes in the body. The results of this study showed that 3-PPA significantly inhibits the synthesis of  $\text{NAD}^+$ , and decreases the expressions of SIRT1 and SIRT3 genes in the myotubes. Therefore, we speculate whether 3-PPA affects myotube acetylation modification through the  $\text{NAD}^+$ -SIRT signaling pathway. Protein acetylation is a post-translational modification of proteins, involving transfer the acetyl-coA and the  $\epsilon$ -amino side chain under the action of acetyltransferase. It plays a regulatory role in stabilizing protein configuration, regulating protein activity and protein interactions. Studies have shown that the role of acetylation and deacetylation in the regulation of skeletal muscle mass may be both condition- and protein-specific [46]. And the acetylation of a lysine residue may block the binding of ubiquitin, thereby reducing the

proteasome-dependent degradation of protein [47, 48]. Consistently, we found that 3-PPA significantly increased the content of acetyl-coA and promoted the acetylation modification of total protein in C2C12, while also leading to a decrease in the ubiquitination of total protein. And C646, an inhibitor of the histone acetyltransferase-CBP/p300 [49], successfully interdicted the effects of 3-PPA in myotube hypertrophy. Acetylation can play a role in the transcriptional expression of some myogenic regulatory factors. Both the acetyltransferase PCAF and p300 promote the acetylation of MyoD, thereby enhancing its transcriptional activity and promoting myoblast differentiation [50]. Pax7 can also be modified by the acetyltransferase MYST1 to regulate acetylation, which plays a key role in the activation of skeletal muscle satellite cells [51]. So next, we want to explore the target of the increasing acetyl-coA.

Foxo is involved in the regulation of cell cycle, metabolism, and protein turnover, and also affects protein ubiquitination [52] and  $\text{NAD}^+$ -SIRT pathway. Some reports demonstrated that NAMPT gene can be targeted by Foxo for transcriptional regulation. Overexpression of Foxo1 can increase the transcription level of NAMPT by 62%, while knocking out Foxo1 reduced the transcription level of NAMPT by 30% [53]. NAMPT also is Foxo3 protein activity regulator, and up-regulation of NAMPT and SIRT1 activity is accompanied by an increase of Foxo3 protein level, which further regulates downstream gene expression [54]. SIRT1 is an important regulatory factor in the upstream of Foxo3. The activity of SIRT1 decreases after dephosphorylation, which affects the deacetylation modification of Foxo3 protein and thus reduces its activity [55]. Additionally, the acetylation of the Foxo3 gene binding region can reduce its ability to activate target gene transcription [56]. Our data showed that 3-PPA significantly reduces Foxo3 protein expression and translocation to the nucleus by inducing its phosphorylation and acetylation. P7C3, an agonist of NAMPT, successfully reverse the effects of 3-PPA on Foxo3, and knockdown of Foxo3 significantly reduces NAMPT gene expression. By using AutoDock 4.0 software, we found 3-PPA can binding with Foxo3 protein directly.

## Conclusion

Based on our observation, we propose that 3-PPA may directly bind to Foxo3 protein, inhibit its activity, and consequently reduce the expression of NAMPT and SIRT gene. Through  $\text{NAD}^+$ /SIRT signaling pathway, it promotes protein acetylation, competitively inhibits ubiquitination, and promotes myotube hypertrophy.

## Abbreviations

ADP	Adenosine diphosphate
AKT	Protein kinase B

ATG5	Autophagy related 5
ATG7	Autophagy related 7
ATP	Adenosine-5'-triphosphate
ATP5A1	ATP synthase alpha-subunit
BNIP3	BCL2 Interacting Protein 3
cAMP	Cyclic adenosine monoPhosphate
cDNA	Complementary DNA
COX6A1	Cytochrome c oxidase subunit 6a1
CT	Cycle threshold
CTX	Cardiotoxin
DEPC	Diethylpyrocarbonate
DMEM	Dulbecco's modified eagle medium
DRP1	Dynamin-related protein 1
EDTA	Ethylenediaminetetraacetic acid
ERK	Extracellular signal-regulated kinase
FADH2	Flavin adenine dinucleotide
Foxo3	Forkhead Box O3
IGF-1	Insulin-like growth factor 1
JAK	Janus kinase
GAS	Gastrocnemius
GRP40	G-protein coupled receptor 40
GRP41	G-protein coupled receptor 41
LD	Lactic acid
mRNA	Messenger ribonucleic acid
mTOR	Mammalian target of rapamycin
MYHC	Myosin heavy chain
MyoD	Myoblast determination protein
MyoG	Myogenin
NAD <sup>+</sup> /NADH	Nicotinamide adenine dinucleotide
NAMPT	Nicotinamide phosphoribosyltransferase
NDUFA6	NADH: ubiquinone oxidoreductase subunit A6
NDUFB8	NADH: ubiquinone oxidoreductase subunit B8
NMNAT2	Nicotinamide mononucleotide adenylyltransferase 2
PARK2	Parkinson protein 2
Pax3	Paired box 3
Pax7	Paired box 7
PBS	Phosphate buffered saline
PCR	Polymerase Chain Reaction
PGC1- $\alpha$	Peroxisome proliferator-activated receptor gamma coactivator 1-alpha
PINK1	PTEN induced putative kinase 1
ROS	Reactive oxygen species
PVDF	Polyvinylidene Fluoride
SDH8	Succinate dehydrogenase subunit 8
SIRT1	Sirtuin 1
SQSTM1	Sequestosome 1
STAT	Signal transducer and activator of transcription
TBST	Tris Buffered Saline + Tween 20
TCA	Tricarboxylic acid cycle
TFAM	Mitochondrial transcription elongation factor
UQCRC1	Cytochrome b-c complex subunit 1
3-PPA	3-Phenylpropionic acid

## Supplementary Information

The online version contains supplementary material available at <https://doi.org/10.1186/s13578-024-01244-2>.

Additional file 1: Fig S1 (a) OD value of CCK-8 to detect proliferation activity of C2C12 (n = 8). (b, c) EdU immunofluorescence images (b) and statistics (c) of proliferative activity of C2C12 cells (n=3). (d) Schematic representation of C2C12 treated with 3-PPA for 6 days. (e, f) Immunofluorescence images (e) and statistics of fusion index (f) of C2C12 myotubes in 3-PPA treatment for 6 days (n = 4). Fig S2 (a–c) Immunoblots (a) and quantification (b, c) of P-STAT3, STAT3, P-JAK2 and JAK2 protein expression of C2C12 myotubes with 3-PPA treatment for 0.5, 1, 3 and 6 h (n=3). (d–f) Immunoblots (d) and quantification (e, f) of P-mTOR, mTOR, P-AKT and AKT protein expression of C2C12 myotubes with 3-PPA treatment for 0.5, 1, 3 and 6 hours (n = 3). (g, h) Immunoblots (g) and quantification (h) of

P-ERK and ERK protein expression of C2C12 myotubes with 3-PPA treatment for 0.5, 1, 3 and 6 h (n = 3). (DOCX 5570 KB)

## Acknowledgements

Not applicable.

## Author contributions

Penglin Li, Pro Qingyan Jiang and Pro Gangshu designed original draft, analyzed data and investigation; Xiaohua Feng, Zewei Ma, and Guli Xu provided experiment resources and methodology; Yexian Yuan, Songbo Wang, Ping Gao and Canjun Zhu were major in supervision; Hongfeng Jiang, Xue Yang and Zewei Ma provided software; Yunlong Zhu and Yujun Wang interpreted the data. Professor Qingyan Jiang and Gang Shu acquired Funding.

## Funding

This work was supported by Double first-class discipline promoting project (2023B10564001); the National Key Research and Development Program (2022YFD1300400); the National Natural Science Foundation of China (32272954); the Local Innovative and Research Teams Project of Guangdong Province (2019BT02N630).

## Availability of data and materials

The data and materials that support the findings of this study are available in the methods of this article.

## Declarations

### Ethics approval and consent to participate

All experimental mice were fed following "The Guidelines for the Care of Laboratory Animals" issued by the Ministry of Science and Technology of the PRC and approved by the Animal Experimentation Committee of South China Agricultural University (Project number SYXK 20220136).

### Consent for publication

Not applicable.

### Competing interests

The authors declare that they have no competing interests.

Received: 9 February 2024 Accepted: 3 May 2024

Published online: 15 May 2024

## References

- Baskin KK, Winders BR, Olson EN. Muscle as a "mediator" of systemic metabolism. *Cell Metab.* 2015;21(2):237–48.
- Li P, Feng J, Jiang H, Feng X, Yang J, Yuan Y, et al. Microbiota derived d-malate inhibits skeletal muscle growth and angiogenesis during aging via acetylation of cyclin a. *EMBO Rep.* 2024;25(2):524–43.
- Kang SH, Lee HA, Kim M, Lee E, Sohn UD, Kim I. Forkhead box O3 plays a role in skeletal muscle atrophy through expression of E3 ubiquitin ligases MuRF-1 and atrogin-1 in cushing's syndrome. *Am J Physiol Endocrinol Metab.* 2017;312(6):E495–e507.
- Gellhaus B, Böker KO, Gsaenger M, Rodenwaldt E, Hüser MA, Schilling AF, et al. Foxo3 knockdown mediates decline of myod1 and myog reducing myoblast conversion to myotubes. *Cells.* 2023. <https://doi.org/10.3390/cells12172167>.
- Soulez M, Tanguay PL, Dô F, Dort J, Crist C, Kotlyarov A, et al. ERK3-MK5 signaling regulates myogenic differentiation and muscle regeneration by promoting FoxO3 degradation. *J Cell Physiol.* 2022;237(4):2271–87.
- Raffaello A, Milan G, Masiero E, Carnio S, Lee D, Lanfranchi G, et al. JunB transcription factor maintains skeletal muscle mass and promotes hypertrophy. *J Cell Biol.* 2010;191(1):101–13.
- Seok YM, Yoo JM, Nam Y, Kim J, Kim JS, Son JH, et al. Mountain ginseng inhibits skeletal muscle atrophy by decreasing muscle RING finger

- protein-1 and atrogin1 through forkhead box O3 in L6 myotubes. *J Ethnopharmacol.* 2021;270: 113557.
8. Jing Y, Zuo Y, Sun L, Yu ZR, Ma S, Hu H, et al. SESN1 is a FOXO3 effector that counteracts human skeletal muscle ageing. *Cell Prolif.* 2023;56(5): e13455.
  9. Yin J, Yang L, Xie Y, Liu Y, Li S, Yang W, et al. Dkk3 dependent transcriptional regulation controls age related skeletal muscle atrophy. *Nat Commun.* 2018;9(1):1752.
  10. Wang LF, Huang CC, Xiao YF, Guan XH, Wang XN, Cao Q, et al. CD38 deficiency protects heart from high fat diet-induced oxidative stress via activating Sirt3/FOXO3 pathway. *Cell Physiol Biochem.* 2018;48(6):2350–63.
  11. Pauline R, Carolina LB, Valentina dE, Brigitte I, David S, Saghi G. SIRT1 deacetylase is essential for hematopoietic stem cell activity via regulation of foxo3. *Blood.* 2012;120(21):2315.
  12. Giron M, Thomas M, Dardevet D, Chassard C, Savary-Auzeloux I. Gut microbes and muscle function: can probiotics make our muscles stronger? *J Cachexia Sarcopenia Muscle.* 2022;13(3):1460–76.
  13. Lahiri S, Kim H, Garcia-Perez I, Reza MM, Martin KA, Kundu P, et al. The gut microbiota influences skeletal muscle mass and function in mice. *Sci Transl Med.* 2019. <https://doi.org/10.1126/scitranslmed.aan5662>.
  14. Grosicki GJ, Fielding RA, Lustgarten MS. Gut microbiota contribute to age-related changes in skeletal muscle size, composition, and function: biological basis for a gut-muscle axis. *Calcif Tissue Int.* 2018;102(4):433–42.
  15. Lefevre C, Bindels LB. Role of the gut microbiome in skeletal muscle physiology and pathophysiology. *Curr Osteoporos Rep.* 2022;20(6):422–32.
  16. Frampton J, Murphy KG, Frost G, Chambers ES. Short-chain fatty acids as potential regulators of skeletal muscle metabolism and function. *Nat Metab.* 2020;2(9):840–8.
  17. Liu Y, Hou Y, Wang G, Zheng X, Hao H. Gut microbial metabolites of aromatic amino acids as signals in host-microbe interplay. *Trend Endocrinol Metab.* 2020;31(11):818–34.
  18. Du L, Qi R, Wang J, Liu Z, Wu Z. Indole-3-propionic acid, a functional metabolite of clostridium sporogenes, promotes muscle tissue development and reduces muscle cell inflammation. *Int J Mol Sci.* 2021. <https://doi.org/10.3390/ijms22212435>.
  19. Agudelo LZ, Ferreira DMS, Dadvar S, Cervenka I, Ketscher L, Izadi M, et al. Skeletal muscle PGC-1 $\alpha$ 1 reroutes kynurenine metabolism to increase energy efficiency and fatigue-resistance. *Nat Commun.* 2019;10(1):2767.
  20. Jang C, Hui S, Zeng X, Cowan AJ, Wang L, Chen L, et al. Metabolite exchange between mammalian organs quantified in pigs. *Cell Metab.* 2019;30(3):594–606.e3.
  21. Kuranov SO, Luzina OA, Onopchenko O, Pishel I, Zozulya S, Gureev M, et al. Exploring bulky natural and natural-like periphery in the design of p-(benzyloxy)phenylpropionic acid agonists of free fatty acid receptor 1 (GPR40). *Bioorganic Chem.* 2020. <https://doi.org/10.1016/j.bioorg.2020.103830>.
  22. Li Z, Liu C, Xu X, Shi W, Li H, Dai Y, et al. Design, synthesis, and biological evaluation of deuterated phenylpropionic acid derivatives as potent and long-acting free fatty acid receptor 1 agonists. *Bioorg Chem.* 2018;76:303–13.
  23. Palanikumar L, Karpauskaitė L, Al-Sayegh M, Chegade I, Alam M, Hassan S, et al. Protein mimetic amyloid inhibitor potentially abrogates cancer-associated mutant p53 aggregation and restores tumor suppressor function. *Nat Commun.* 2021;12(1):3962.
  24. Sartori R, Romanello V, Sandri M. Mechanisms of muscle atrophy and hypertrophy: implications in health and disease. *Nat Commun.* 2021;12(1):330.
  25. Choi S, Jeong HJ, Kim H, Choi D, Cho SC, Seong JK, et al. Skeletal muscle-specific Prmt1 deletion causes muscle atrophy via deregulation of the PRMT6-FOXO3 axis. *Autophagy.* 2019;15(6):1069–81.
  26. Eijkelenboom A, Burgering BM. FOXOs: signalling integrators for homeostasis maintenance. *Nat Rev Mol Cell Biol.* 2013;14(2):83–97.
  27. Winbanks CE, Weeks KL, Thomson RE, Sepulveda PV, Beyer C, Qian H, et al. Follistatin-mediated skeletal muscle hypertrophy is regulated by Smad3 and mTOR independently of myostatin. *J Cell Biol.* 2012;197(7):997–1008.
  28. Hwang SY, Sung B, Kim ND. Roles of folate in skeletal muscle cell development and functions. *Arch Pharmacol Res.* 2019;42(4):319–25.
  29. Zammit PS. Function of the myogenic regulatory factors Myf5, MyoD, Myogenin and MRF4 in skeletal muscle, satellite cells and regenerative myogenesis. *Semin Cell Dev Biol.* 2017;72:19–32.
  30. Kovanda A, Režen T, Rogelj B. MicroRNA in skeletal muscle development, growth, atrophy, and disease. *Wiley Interdiscip Rev RNA.* 2014;5(4):509–25.
  31. Walsh ME, Bhattacharya A, Sataranatarajan K, Qaisar R, Sloane L, Rahman MM, et al. The histone deacetylase inhibitor butyrate improves metabolism and reduces muscle atrophy during aging. *Aging Cell.* 2015;14(6):957–70.
  32. Russell WR, Duncan SH, Scobbie L, Duncan G, Cantlay L, Calder AG, et al. Major phenylpropanoid-derived metabolites in the human gut can arise from microbial fermentation of protein. *Mol Nutr Food Res.* 2013;57(3):523–35.
  33. Amaresh CP, Kotb A, Je-Hyun Y, Jennifer LM, Xiaoling Y, Jessica C, et al. RNA-binding protein AUF1 promotes myogenesis by regulating MEF2C expression levels. *Mol Cell Biol.* 2014;34(16):3106–19.
  34. Yaping N, Hu C, Cilin G, Zhuning Y, Xingyu Z, Xumeng Z, et al. Palmdelphin promotes myoblast differentiation and muscle regeneration. *Sci Rep.* 2017;7(1):41608.
  35. Bo L, Nan L, Yuling J, Chao L, Le M, Cong W, et al. Effects of excessive retinoic acid on C2C12 myogenesis. *J Hard Tissue Biol.* 2016;25(2):97–103.
  36. Sun Young P, Georgia K, Hugo RR, Hong S. Effects of energy drinks on myogenic differentiation of murine C2C12 myoblasts. *Sci Rep.* 2023;13(1):8481.
  37. Woodall BP, Woodall MC, Luongo TS, Grisanti LA, Tilley DG, Elrod JW, et al. Skeletal muscle-specific G protein-coupled receptor kinase 2 ablation alters isolated skeletal muscle mechanics and enhances clenbuterol-stimulated hypertrophy. *J Biol Chem.* 2016;291(42):21913–24.
  38. Attwaters M, Hughes SM. Cellular and molecular pathways controlling muscle size in response to exercise. *FEBS J.* 2022;289(6):1428–56.
  39. Wahlström A, Sayin SI, Marschall HU, Bäckhed F. Intestinal crosstalk between bile acids and microbiota and its impact on host metabolism. *Cell Metab.* 2016;24(1):41–50.
  40. Pan JH, Kim JH, Kim HM, Lee ES, Shin DH, Kim S, et al. Acetic acid enhances endurance capacity of exercise-trained mice by increasing skeletal muscle oxidative properties. *Biosci Biotechnol Biochem.* 2015;79(9):1535–41.
  41. Nishida Y, Nawaz A, Kado T, Takikawa A, Igarashi Y, Onogi Y, et al. Astaxanthin stimulates mitochondrial biogenesis in insulin resistant muscle via activation of AMPK pathway. *J Cachexia Sarcopenia Muscle.* 2020;11(1):241–58.
  42. Lv H, Lv G, Chen C, Zong Q, Jiang G, Ye D, et al. NAD(+) metabolism maintains inducible PD-L1 expression to drive tumor immune evasion. *Cell Metab.* 2021;33(1):110–27.e5.
  43. Yao H, Liu M, Wang L, Zu Y, Wu C, Li C, et al. Discovery of small-molecule activators of nicotinamide phosphoribosyltransferase (NAMPT) and their preclinical neuroprotective activity. *Cell Res.* 2022;32(6):570–84.
  44. Basse AL, Agerholm M, Farup J, Dalbram E, Nielsen J, Ørtenblad N, et al. Nampt controls skeletal muscle development by maintaining Ca(2+) homeostasis and mitochondrial integrity. *Mol Metab.* 2021;53: 101271.
  45. Døllerup OL, Chubanava S, Agerholm M, Søndergård SD, Altıntaş A, Møller AB, et al. Nicotinamide riboside does not alter mitochondrial respiration, content or morphology in skeletal muscle from obese and insulin-resistant men. *J Physiol.* 2020;598(4):731–54.
  46. Alamdari N, Aversa Z, Castillero E, Hasselgren PO. Acetylation and deacetylation—novel factors in muscle wasting. *Metabolism.* 2013;62(1):1–11.
  47. Zhang N, Zhang Y, Wu B, Wu S, You S, Lu S, et al. Deacetylation-dependent regulation of PARP1 by SIRT2 dictates ubiquitination of PARP1 in oxidative stress-induced vascular injury. *Redox Biol.* 2021;47: 102141.
  48. Caron C, Boyault C, Khochbin S. Regulatory cross-talk between lysine acetylation and ubiquitination: role in the control of protein stability. *BioEssays.* 2005;27(4):408–15.
  49. Bai B, Zhang Q, Wan C, Li D, Zhang T, Li H. CBP/p300 inhibitor C646 prevents high glucose exposure induced neuroepithelial cell proliferation. *Birth Defect Res.* 2018;110(14):1118–28.
  50. Moresi V, Marroncelli N, Coletti D, Adamo S. Regulation of skeletal muscle development and homeostasis by gene imprinting, histone acetylation and microRNA. *Biochem Biophys Acta.* 2015;1849(3):309–16.
  51. Sincennes MC, Brun CE, Lin AYT, Rosembert T, Datzkiw D, Saber J, et al. Acetylation of PAX7 controls muscle stem cell self-renewal and differentiation potential in mice. *Nat Commun.* 2021;12(1):3253.
  52. Milan G, Romanello V, Pescatore F, Armani A, Paik JH, Frasson L, et al. Regulation of autophagy and the ubiquitin-proteasome system by the

- FoxO transcriptional network during muscle atrophy. *Nat Commun.* 2015;6:6670.
53. Tao R, Wei D, Gao H, Liu Y, DePinho RA, Dong XC. Hepatic FoxOs regulate lipid metabolism via modulation of expression of the nicotinamide phosphoribosyltransferase gene. *J Biol Chem.* 2011;286(16):14681–90.
  54. Wang B, Hasan MK, Alvarado E, Yuan H, Wu H, Chen WY. NAMPT overexpression in prostate cancer and its contribution to tumor cell survival and stress response. *Oncogene.* 2011;30(8):907–21.
  55. Yao J, Wang J, Xu Y, Guo Q, Sun Y, Liu J, et al. CDK9 inhibition blocks the initiation of PINK1-PRKN-mediated mitophagy by regulating the SIRT1-FOXO3-BNIP3 axis and enhances the therapeutic effects involving mitochondrial dysfunction in hepatocellular carcinoma. *Autophagy.* 2022;18(8):1879–97.
  56. Tang G, Du Y, Guan H, Jia J, Zhu N, Shi Y, et al. Butyrate ameliorates skeletal muscle atrophy in diabetic nephropathy by enhancing gut barrier function and FFA2-mediated PI3K/Akt/mTOR signals. *Br J Pharmacol.* 2022;179(1):159–78.

### **Publisher's Note**

Springer Nature remains neutral with regard to jurisdictional claims in published maps and institutional affiliations.